Alanine-scanning mutagenesis of the small-subunit beta A-beta B loop of chloroplast ribulose-1,5-bisphosphate carboxylase/oxygenase: substitution at Arg-71 affects thermal stabilit...

ARTICLE *in* BIOCHEMISTRY · MAY 2001

Impact Factor: 3.02 · Source: PubMed

4 AUTHORS, INCLUDING:

Maria Gloria Esquivel
Technical University of Lisbon
35 PUBLICATIONS **296** CITATIONS

SEE PROFILE

Alanine-Scanning Mutagenesis of the Small-Subunit βA−βB Loop of Chloroplast Ribulose-1,5-Bisphosphate Carboxylase/Oxygenase: Substitution at Arg-71 Affects Thermal Stability and CO_2/O_2 Specificity†

Robert J. Spreitzer,*,‡ Maria G. Esquivel,§ Yu-Chun Du,‡ and Patrick D. McLaughlin‡

Department of Biochemistry, University of Nebraska, Lincoln, Nebraska 68588, and Department of Botany and Biological Engineering, Technical University of Lisbon, P-1399 Lisbon, Portugal

Received December 27, 2000

ABSTRACT: Ribulose-1,5-bisphosphate carboxylase/oxygenase (Rubisco) enzymes from different species differ with respect to carboxylation catalytic efficiency and CO_2/O_2 specificity, but the structural basis for these differences is not known. Whereas much is known about the chloroplast-encoded large subunit, which contains the α/β-barrel active site, much less is known about the role of the nuclear-encoded small subunit in Rubisco structure and function. In particular, a loop between β-strands A and B contains 21 or more residues in plants and green algae, but only 10 residues in prokaryotes and nongreen algae. To determine the significance of these additional residues, a mutant of the green alga *Chlamydomonas reinhardtii*, which lacks both small-subunit genes, was used as a host for transformation with directed-mutant genes. Although previous studies had indicated that the βA−βB loop was essential for holoenzyme assembly, Ala substitutions at residues conserved among land plants and algae (Arg-59, Tyr-67, Tyr-68, Asp-69, and Arg-71) failed to block assembly or eliminate function. Only the Arg-71 → Ala substitution causes a substantial decrease in holoenzyme thermal stability. Tyr-68 → Ala and Asp-69 → Ala enzymes have lower $K_m(CO_2)$ values, but these improvements are offset by decreases in carboxylation V_{max} values. The Arg-71 → Ala enzyme has a decreased carboxylation V_{max} and increased $K_m(CO_2)$ and $K_m(O_2)$ values, which account for an observed 8% decrease in CO_2/O_2 specificity. Despite the fact that Arg-71 is more than 20 Å from the large-subunit active site, it is apparent that the small-subunit βA−βB loop region can influence catalytic efficiency and CO_2/O_2 specificity.

Ribulose-1,5-bisphosphate carboxylase/oxygenase (Rubisco,[1] EC 4.1.1.39) plays an essential role for the existence of life on our planet. It fixes atmospheric CO_2 in the first reaction of the Calvin cycle of photosynthesis by catalyzing the reaction between unbound, gaseous CO_2 and RuBP to form two molecules of 3-phosphoglycerate (for reviews, see refs *1* and *2*). Net CO_2 fixation is limited by Rubisco due to the fact that the enzyme has a k_{cat} for carboxylation of only a few per second. Furthermore, O_2 is mutually competitive with CO_2 at the same active site, and the enzyme catalyzes the oxygenation of RuBP to produce phosphoglycerate and phosphoglycolate (*3*). This latter, nonessential product enters the photorespiratory pathway, which subsequently generates CO_2 during the conversion of glycine to serine. Thus, net CO_2 fixation is defined by the velocity of carboxylation minus half the velocity of oxygenation, whereas CO_2/O_2 specificity is defined by the kinetic constant Ω, which is equal to V_cK_o/V_oK_c, where V is the V_{max} of carboxylation or oxygenation and K is the Michaelis constant for O_2 or CO_2 (*4*, *5*). There has been much interest in engineering Rubisco to increase the level of carboxylation or decrease the level of oxygenation as a means of increasing the production of food, fiber, and energy (*1*, *2*, *6*, *7*).

The Rubisco holoenzyme of land plants and green algae is comprised of eight 55 kDa large subunits, encoded by the chloroplast *rbcL* gene, and eight 15 kDa small subunits, encoded by a family of nearly identical *RbcS* nuclear genes (for a review, see ref *2*). Much is known about the structure−function relationships of the large subunit (for reviews, see refs *6* and *7*). It contains the active site. Numerous X-ray crystal structures of both prokaryotic and eukaryotic holoenzymes have identified specific residues at the surface of the α/β-barrel domain of one large subunit and residues in the N-terminal domain of a neighboring large subunit that interact with each other and with the transition state analogue 2-carboxy-D-arabinitol 1,5-bisphosphate (*8*−*11*). The essentiality and role of many of these catalytic residues and their neighboring large-subunit regions have been defined by biochemical and genetic methods, primarily with the aid of prokaryotic Rubisco expressed in *Escherichia coli* (for a review, see ref *6*) or by screening, selection, and chloroplast transformation in the green algae *Chlamydomonas reinhardtii* (for a review, see ref *12*).

† This work is supported by Grant DE-FG03-00ER15044 from the U.S. Department of Energy and by the Nebraska Agricultural Research Division (Journal Series Paper 13219).

* To whom correspondence should be addressed. E-mail: rspreitzer1@unl.edu. Telephone: (402) 472-5446. Fax: (402) 472-7842.

‡ University of Nebraska.

§ Technical University of Lisbon.

[1] Abbreviations: Rubisco, D-ribulose-1,5-bisphosphate carboxylase/oxygenase; RuBP, D-ribulose 1,5-bisphosphate; V_c, V_{max} for carboxylation; V_o, V_{max} for oxygenation; K_c, Michaelis constant for CO_2; K_o, Michaelis constant for O_2; Ω, CO_2/O_2 specificity factor; SDS, sodium dodecyl sulfate; kb, kilobase.

10.1021/bi002943e CCC: $20.00
Published on Web 04/18/2001

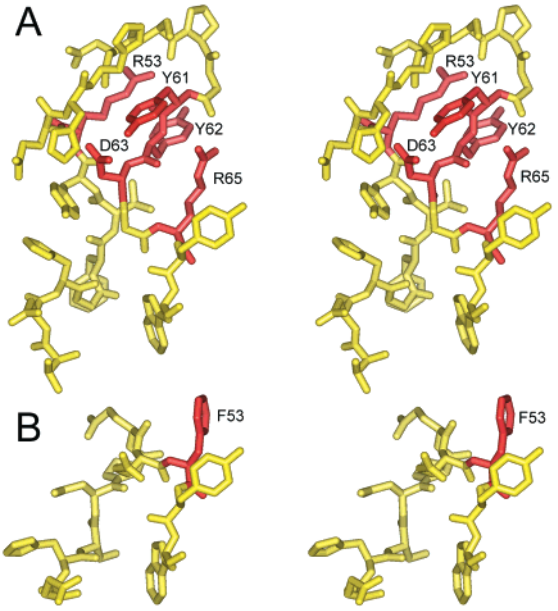

FIGURE 1: Stereoimages of the Rubisco small-subunit βA−βB loop. (A) The loop in spinach Rubisco (8RUC) contains 22 residues (*8*), five of which (in red) are conserved among land plants and green algae but are missing or different from the small subunits of prokaryotes and nongreen algae. (B) The loop in *Synechococcus* Rubisco (1RBL) contains only 10 residues (*10*), one of which (in red) may be the structural homologue of spinach Arg-65.

GREEN ALGAE			
Chlamydomonas	39-	IPCLEFAEADKAYVSNESAIRFGSVSCLYYDNRYWTMW	-80
Euglena	39-	SPCLEFAAPENSFIANDNTVRFSGTAAGYYDNRYWTMW	-80
Acetabularia	39-	TPCLEFAASDQAYAGNENCIRMGPVASTYQDNRYWTMW	-80
LAND PLANTS			
Spinacea	39-	VPCLEFETDHGFVY REHHNSPGYYDGRYWTMW	-70
Pisum	39-	VPCLEFELEKGFVY REHNKSPGYYDGRYWTMW	-70
Nicotiana	39-	VPCLEFETEHGFVY RENNKSPGYYDGRYWTMW	-70
Zea	39-	IPCLEFESKVGFVY RENSTSPCYYDGRYWTMW	-69
Glycine	39-	IPCLEFELEHGHVY REHNRSLGYYDGRYWTMW	-70
Helianthus	39-	VPCLEFELEHGFVY RENARSPGYYDGRYWTMW	-70
Mesembryanthemum	39-	VPCLEFEPTHGFVY REHGNTPGYYDGRYWTMW	-70
Gossypium	39-	IPCLEFELEEGFVH RKYSSLPTYYDGRYWTMW	-70
Cucumis	39-	VPCVEFDIGSGFVY RENHRSPGFYDGRYWTMW	-70
Amaranthus	39-	IPCIEFELEHPFVY RENHRSPGYQDGRYWTMW	-70
Brassica	39-	IPCVEFELEHGFVY REHGSTPGYYDGRYWTMW	-70
Arabidopsis	39-	IPCVEFELEHGFVY REHGNTPGYYDGRYWTMW	-70
Triticum	39-	VPCLEFSKVGFVF REHNSSPGYYDGRYWTMW	-69
Lemna	39-	VPCIEFSKEGFVY RENHASPGYYDGRYWTMW	-69
Pteris	39-	TPCIEFDTIGSVY REHFHGSGYYDGRYWIMW	-69
Marchantia	39-	APCIEFDVQGTVT REGSTMPGYYDGRYWTMW	-69
NONGREEN ALGAE			
Galdieria partita	32-	AIGIEYTNDIHPRN AYWEIW	-51
Cyanidium	32-	ALSVEYTDDPHPRN SYWEMW	-51
Porphyridium	32-	AVSVEYTDDPHPRN SFWELW	-51
Cylindrotheca	32-	AMNVEWTDDPHPRN NYWELW	-51
PROKARYOTES			
Synechococcus	39-	HPLIEFNEHSNPEE FYWTMW	-58
Anabaena	38-	IPAVEFNEVSEPTE LYWTLW	-57
Alcaligenes	32-	AVGLEYTDDPHPRN TYWEMF	-51
Rhodobacter	32-	AVSLEHTDDPHPRN TYWEMW	-51
Chromatium	46-	NPAIEHTEPENAFD HYWYMW	-65

FIGURE 2: Sequences of small-subunit βA−βB loop regions. Sequences were chosen from the National Center for Biotechnology Information Entrez Protein Database to illustrate the diversity of residue identities, and were aligned relative to existing X-ray crystal structures (*8*−*11*). Residues conserved among land plants and green algae but missing or different from the small subunits of prokaryotes and nongreen algae are underlined. β-Strands A and B are shaded in gray.

Rubisco holoenzymes from various species differ with respect to k_{cat} (1−10 s^{-1}) and Ω (10−240) (*2*, *13*−*15*), but the large-subunit catalytic residues are conserved among more than 1000 deduced sequences (*16*). In contrast, the hundreds of known small-subunit sequences are more divergent than those of the large subunit, and some Rubisco enzymes of prokaryotes and dinoflagelates, which have Ω values of <40 (*13*, *17*), lack small subunits entirely. Nonetheless, the role of the small subunit in Rubisco structure and function remains mysterious (for a review, see ref *2*).

It has been difficult to study the small subunits of land plants because they are encoded by a family of *RbcS* genes that cannot be replaced or eliminated (*2*, *18*). Furthermore, it has not been possible to assemble the large and small subunits of eukaryotic Rubisco in *E. coli* (*19*), precluding the use of in vitro-directed mutagenesis. However, the most notable difference among small subunits concerns the larger loop between β-strands A and B that is characteristic of land-plant small subunits (Figure 1) (*8*−*10*). The small subunits of land plants and green algae contain 21 or more residues between β-strands A and B, but those of prokaryotes and nongreen algae contain 10 residues (Figure 2). To examine the significance of this land-plant loop, Wasmann et al. (*20*) used in vitro transcription and translation to generate altered small subunits, and studied their ability to assemble with large subunits after transport into isolated pea chloroplasts. Whereas cyanobacterial small subunits could not assemble with pea large subunits, they could be made assembly-competent by replacing the 10-residue βA−βB loop with the longer loop (22 residues) characteristic of land plants (*20*). Subsequent directed mutagenesis studies revealed that an R53E substitution in the pea small subunit (Figure 2) could block holoenzyme assembly (*21*, *22*), further indicating that the βA−βB loop might be essential for the assembly of the eukaryotic holoenzyme. Although a number of additional small-subunit substitutions were created and examined that did not block holoenzyme assembly (*21*), their influence on the function of Rubisco could not be determined due to the low yield of holoenzyme from isolated chloroplasts. More recently, genetic screening and selection in *Chlamydomonas* identified N54S and A57V substitutions in the small-subunit βA−βB loop (Figure 2) that can complement an L290F mutant substitution in the Rubisco large subunit (*23*, *24*). These small-subunit substitutions increase Ω and V_c of the mutant enzyme back to near normal levels, indicating that the βA−βB loop may also contribute to holoenzyme catalytic efficiency.

Recent insertional mutagenesis experiments in *Chlamydomonas* produced a mutant strain that lacks the 13 kb locus that encodes both members of the *RbcS* gene family (*25*). Like photosynthesis-deficient mutants of *Chlamydomonas* in general (*12*, *26*), this *RbcS*Δ strain can be maintained when supplied with acetate as an alternative carbon source. It can be restored to photosynthetic competence via transformation with either of the two *RbcS* genes (*RbcS1* or *RbcS2*) (*25*). Therefore, it is now possible to examine the role of the eukaryotic small subunit in the structure and function of Rubisco. To further assess the significance of the small-subunit βA−βB loop, directed mutagenesis and transformation were used to replace five conserved residues with Ala (Figures 1 and 2). None of these residues was found to be essential for holoenzyme assembly, but one substitution influences both Ω and carboxylation V_{max}.

MATERIALS AND METHODS

Strains and Culture Conditions. *C. reinhardtii* 2137 mt^+ was the wild-type strain (*26*). The *RbcS*Δ-T60-3 mt^- strain

was used as the host for transformation. It lacks photosynthesis and requires acetate for growth due to deletion of the 13 kb locus that contains *RbcS1* and *RbcS2* (*25*). All strains are maintained at 25 °C in darkness on medium containing 10 mM acetate and 1.5% Bacto agar (*26*). For biochemical analysis, cells were grown in 250−500 mL of liquid acetate medium at 25 °C on a rotary shaker at 120 rpm in darkness.

Directed Mutagenesis and Transformation. Plasmid pSS1 (*25*), which is comprised of pUC19 (*27*) and a 5 kb *Eco*RI fragment containing the entire *Chlamydomonas RbcS1* gene (*28*), was used for directed mutagenesis and transformation. Mutagenesis was performed with synthetic oligonucleotides and a kit from Pharmacia (*29*). Plasmids were propagated in *E. coli* XL1-Blue cells (Stratagene). The amino acid substitutions arising from changes in codons were as follows: R59A (CGC → GCC), R59E (CGC → GAG), Y67A (TAC → GCC), Y68A (TAC → GCC), D69A (GAC → GCC), and R71A (CGC → GCC). For transformation of the *Chlamydomonas RbcS*Δ strain, cells were grown in 50 mL of liquid acetate medium in darkness to a density of 2×10^6 cells/mL. The cells were concentrated to 4×10^7 cells in 0.4 mL of minimal growth medium (without acetate) containing 5% polyethylene glycol, and transformed with plasmid DNA (3 μg) by the glass-bead vortexing method (*30*). Transformed cells were recovered by selecting for photosynthetic competence (1×10^7 cells per 100 mm Petri plate) on minimal medium in the light (80 μeinsteins m^{-2} s^{-1}) at 25 °C (*25*). By employing standard procedures (*24*, *25*), we purified DNA from the transformants, amplified *RbcS1* by the polymerase chain reaction, and confirmed the presence of the expected mutations by DNA sequencing.

Biochemical Analysis. Approximately 1×10^9 cells were harvested by centrifugation and sonicated in 50 mM *N*,*N*-bis(2-hydroxyethyl)glycine (pH 8.0), 10 mM $NaHCO_3$, 10 mM $MgCl_2$, and 1 mM dithiothreitol at 0 °C for 1.5 min (*31*). Protein was quantified (*32*) and subjected to SDS−polyacrylamide gel electrophoresis (*33*) and Western blotting with rabbit anti-tobacco Rubisco immunoglobulin G (*34*), or fractionated on sucrose gradients as the means of purifying Rubisco holoenzyme (*31*). RuBP carboxylase and oxygenase activities and kinetic constants were measured via the incorporation of acid-stable ^{14}C from $NaH^{14}CO_3$ (*23*). Ω of purified and activated Rubisco (20 μg/reaction) was determined by assaying carboxylase and oxygenase activities simultaneously with 130 μM [1-^{3}H]RuBP (9.7 Ci/mol) and 2 mM $NaH^{14}CO_3$ (5 Ci/mol) in 30 min reactions at 25 °C (*35*, *36*). The [1-^{3}H]RuBP and phosphoglycolate phosphatase used in these assays were synthesized and/or purified according to standard methods (*35*, *37*). Rubisco thermal stability was assayed by incubating purified and activated enzymes (5 μg) in 0.5 mL of 50 mM *N*,*N*-bis(2-hydroxyethyl)glycine (pH 8.0), 10 mM $NaHCO_3$ (2 Ci/mol), and 10 mM $MgCl_2$ at various temperatures for 10 min (*24*, *38*). The samples were then cooled on ice for 5 min, and carboxylase activity was initiated at 25 °C by adding 20 μL of 10 mM RuBP. After 1 min, the reactions were terminated with 0.5 mL of 3 M formic acid in methanol.

RESULTS

Recovery and Phenotypes of Mutants. Although the *Chlamydomonas* βA−βB loop is six residues longer than the land-plant βA−βB loop, alignment of 197 small-subunit sequences revealed that there are five residues in the βA−βB loops of land-plant and *Chlamydomonas* small subunits that are absent or different from the residues in the βA−βB loops of prokaryotes and nongreen algae (Figure 2). In an attempt to test the functional significance of these residues (Arg-59, Tyr-67, Tyr-68, Asp-69, and Arg-71) without drastically altering holoenzyme structure, single mutations were created in the *Chlamydomonas RbcS1* gene that would cause each of the residues to be substituted with Ala. When these *RbcS1* mutant genes were transformed into the *Chlamydomonas RbcS*Δ deletion mutant, each restored photosynthetic ability. Thus, none of the residues plays an essential role in Rubisco function or assembly. When growth was compared on solid minimal medium (without acetate) at 25 °C (*26*), all of the mutant strains were indistinguishable from a strain transformed with the wild-type *RbcS1* gene (*25*). However, in contrast to the other strains, mutant R71A was unable to grow on minimal medium at 35 °C.

In previous studies, when Arg-53 of the pea small subunit was replaced with Glu, small subunits failed to assemble (*20*) or assembled at a substantially reduced rate (*21*) with large subunits in isolated pea chloroplasts. Because Arg-53 of pea was assumed to be homologous with Arg-59 of *Chlamydomonas* on the basis of sequence alignment (Figure 2), finding that the *Chlamydomonas* R59A mutant strain could grow photosynthetically was somewhat unexpected. To further test whether Arg-59 (*Chlamydomonas*) and Arg-53 (pea) are homologous residues with regard to βA−βB loop structure, an *RbcS1* mutation was created that would produce an R59E substitution. Once again, photosynthesis-competent transformants were recovered when the *RbcS1*-R59E gene was transformed into the *RbcS*Δ deletion strain. However, the R59E mutant cells grew substantially slower than wild-type *RbcS1* transformants on minimal medium at 25 °C, and failed to grow on minimal medium at 35 °C. Thus, Arg-59 (*Chlamydomonas*) and Arg-53 (land plants) are likely to be homologous residues (Figure 2), but it is the presence of Glu rather than the absence of Arg that may be detrimental to holoenzyme assembly or stability.

To determine whether the temperature-conditional, photosynthesis-deficient phenotypes of R59E and R71A resulted from a lack of holoenzyme at the 35 °C restrictive temperature, Western analysis was performed on protein extracts of cells grown at both 25 and 35 °C with acetate medium in darkness. Whereas both of the mutants grow as well as the wild type under these conditions, R59E has substantially less Rubisco at 25 °C, and both mutants lack holoenzyme at 35 °C (Figure 3).

Thermal Stability of Mutant Rubisco Enzymes. Because nuclear transformation of *Chlamydomonas* occurs by nonhomologous recombination (*30*), the level of expression of an introduced gene might be influenced by its location in the genome. However, except for mutants R59E and R71A (Figure 3), none of the mutants had substantially less holoenzyme than wild-type *RbcS1* transformants when Rubisco was purified from extracts of cells grown at 25 °C in darkness (data not shown). Therefore, no structural instability of the R59A, Y67A, Y68A, and D69A mutant enzymes was apparent in vivo. In contrast, only trace amounts of the R59E holoenzyme could be isolated from sucrose gradients, precluding a detailed biochemical analysis

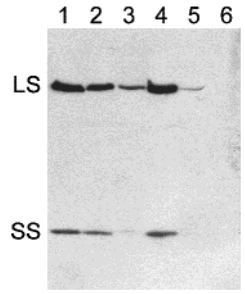

FIGURE 3: Western blot analysis of total soluble proteins from the wild type (lanes 1 and 4), mutant *RbcS1*-R71A (lanes 2 and 5), and mutant *RbcS1*-R59E (lanes 3 and 6). Extracts (30 μg/lane) of cells grown at 25 (lanes 1−3) or 35 °C (lanes 4−6) with acetate medium in darkness were fractionated by SDS−polyacrylamide (7.5 to 15%) gradient gel electrophoresis. Proteins were blotted to nitrocellulose, probed with anti-Rubisco immunoglobulin G (0.5 μg/mL), and detected by enhanced chemiluminescence (*34*). The Rubisco large subunit (LS) and small subunit (SS) are denoted.

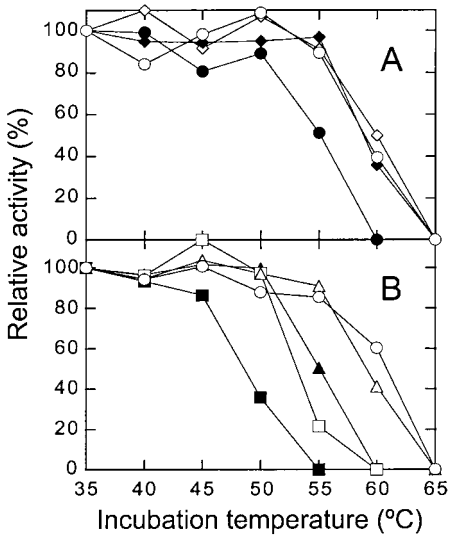

FIGURE 4: Thermal inactivation of Rubisco purified from wild-type strains and *RbcS1* mutants. Rubisco was incubated at each temperature for 10 min. The samples were then cooled on ice, and RuBP carboxylase activity was assayed at 25 °C. Activities were normalized against activity measured after the 35 °C incubation. (A) Wild type (○), transformant containing only the wild-type *RbcS1* gene (◇), transformant containing only the wild-type *RbcS2* gene (◆), and mutant R59A (●). (B) Wild type (○), mutant R71A (■), mutant Y68A (□), mutant Y67A (▲), mutant D69A (△).

of the properties of this mutant enzyme.

To further explore the role of the βA−βB loop in holoenzyme stability, one can examine the thermal stability of each of the purified mutant enzymes in vitro (*24*, *38*). Because the mutant enzymes contain only *RbcS1*-encoded small subunits, it was first important to determine whether there was any difference in thermal stability between the wild-type holoenzyme and holoenzymes containing only the *RbcS1*- or *RbcS2*-encoded small subunits (*25*). As shown in Figure 4A, no difference in thermal stability was found between these enzyme forms. Considering that the R59E substitution appears to have a dramatic effect on holoenzyme stability in *Chlamydomonas* (Figure 3) and land plants (*21*, *22*), we anticipated that the R59A enzyme might also have an associated thermal instability. However, this mutant holoenzyme was only moderately less stable than wild-type Rubisco in vitro (Figure 4A). Furthermore, the Y67A and Y68A holoenzymes were not significantly different from the

Table 1: Oxygen Inhibition of RuBP Carboxylase Specific Activity for Purified Wild-Type and Mutant Rubisco Enzymes

	activity [μM CO_2 h^{-1} (mg of protein)$^{-1}$][a]			
enzyme	100% N_2 with 12.4 mM $NaHCO_3$	100% N_2 with 0.98 mM $NaHCO_3$ (A)	100% O_2 with 0.98 mM $NaHCO_3$ (B)	ratio (A/B)
wild type	113 ± 8	26.9 ± 1.5	9.7 ± 0.4	2.8
R59A	127 ± 8	29.4 ± 0.5	9.8 ± 0.5	3.0
Y67A	89 ± 5	22.4 ± 1.7	7.3 ± 0.4	3.1
Y68A	46 ± 1	10.9 ± 0.7	3.9 ± 0.2	2.8
D69A	48 ± 11	13.6 ± 0.3	4.5 ± 0.3	3.0
R71A	18 ± 1	3.5 ± 0.5	1.4 ± 0.2	2.5

[a] Values are means ± standard deviation of triplicate assays of a single enzyme preparation.

Table 2: Kinetic Properties of Rubisco Purified from the Wild Type and Mutants

kinetic constant	wild type	Y68A	D69A	R71A
$\Omega = V_cK_o/V_oK_c$[a]	61 ± 1	60 ± 1	60 ± 1	56 ± 1
V_c (μmol h^{-1} mg^{-1})[a]	152 ± 8	44 ± 8	66 ± 17	24 ± 6
K_c (μM CO_2)[a]	34 ± 2	24 ± 1	22 ± 1	44 ± 5
K_o (μM O_2)[a]	537 ± 44	501 ± 19	459 ± 38	900 ± 117
V_c/K_c[b]	4.5	1.8	3.0	0.5
K_o/K_c[b]	16	21	21	20
V_c/V_o[b]	3.8	2.9	2.9	2.8

[a] Values are means ± standard deviation of three separate enzyme preparations. [b] Calculated values.

R59A holoenzyme with regard to thermal stability (compare panels A and B of Figure 4), and the D69A holoenzyme was not significantly different from the wild-type enzyme (Figure 4B). Only the R71A substitution had a substantial effect on holoenzyme thermal stability in vitro, which is consistent with the temperature-conditional, photosynthesis-deficient phenotype of the R71A mutant strain (Figure 3). Wild-type Rubisco retained more than 90% of its carboxylase activity after a 10 min incubation at 55 °C, but the R71A enzyme was completely inactivated (Figure 4B).

Kinetics of the Mutant Enzymes. To determine whether the conserved residues in the βA−βB loop might play a role in catalytic efficiency or CO_2/O_2 specificity, each of the purified mutant enzymes was initially examined for carboxylation specific activity and O_2 inhibition of this activity (Table 1) (*23*). When assayed with saturating CO_2 (12.4 mM $NaHCO_3$) in the absence of O_2 (100% N_2), the Y68A, D69A, and R71A mutant enzymes had less than half the wild-type level of carboxylase activity. When assayed with limiting CO_2 (0.98 mM $NaHCO_3$) in the absence (100% N_2) and presence (100% O_2) of oxygen, only the R71A mutant enzyme had a decrease in the ratio of these two measurements of carboxylase activity. It would seem from this lower ratio that the R71A enzyme has greater specificity for CO_2 (i.e., less O_2 inhibition of carboxylase activity), but it is important to point out that the ratio (R) of carboxylase activities under 100% N_2 and 100% O_2 is, in fact, determined by only the K_m values for CO_2 and O_2 according to the relationship $R = 1 + K_c[O_2]/K_o(K_c + [CO_2])$ (*23*). Nonetheless, because the Y68A, D69A, and R71A mutant enzymes appeared to have significant alteration in enzyme function, they were deemed appropriate for further, more detailed kinetic analysis.

As shown in Table 2, the Y68A and D69A enzymes have quite similar kinetic constants. Relative to the wild-type

enzyme, both have lower K_c and higher K_o/K_c values, but these beneficial alterations do not improve carboxylation catalytic efficiency (V_c/K_c) or Ω because both enzymes have >55% decreases in V_c. In contrast to the Y68A and D69A enzymes, the R71A mutant enzyme has an 8% decrease in Ω relative to the wild-type enzyme (Table 2). This decrease in Ω results from >80% decreases in V_c and V_c/K_c despite an increase in K_o/K_c comparable to that seen in the Y68A and D69A mutant enzymes. The increase in K_o/K_c of the R71A mutant enzyme results from a nearly 2-fold increase in K_o, which is primarily responsible for the decrease in the level of O_2 inhibition of carboxylase observed with limiting CO_2 (Table 1) (*23*).

DISCUSSION

Because the Rubisco small subunits of *Chlamydomonas* and spinach are only 44% identical in primary structure, it was somewhat unexpected to find that Ala substitutions at five of the most conserved residues in land-plant and green-algal small subunits (Figure 2) did not eliminate Rubisco function or substantially impair photosynthesis in vivo. The small decreases in the levels of carboxylation (Tables 1 and 2) and holoenzyme stability (Figures 3 and 4) brought about by the Ala replacements must be of sufficient functional significance to account for the retention of the conserved residues during evolution. Because these residues are identical in *Chlamydomonas* and spinach Rubisco (Figure 2), they cannot account for differences in catalysis between the *Chlamydomonas* and spinach enzymes. However, small subunits of prokaryotes and nongreen algae lack these particular residues, primarily due to the absence of 11 or more residues that are characteristic of the small-subunit βA−βB loops of plants and green algae (Figures 1 and 2). Thus, differences in catalysis observed between prokaryotic or nongreen-algal and land-plant or green-algal Rubisco enzymes could, in part, be due to the substantial differences in their βA−βB loops. Other changes in holoenzyme structure may also have occurred during phylogenetic divergence that complement (compensate for) these structural differences.

Previous studies had indicated that the longer βA−βB loop of land plants might be essential for the assembly of the land-plant holoenzyme (*20*). However, when a number of amino acid substitutions were examined in the pea βA−βB loop (R53E, E54R, H55A, P59A, D63G, D63L, and Y66A) (*21*), only one (R53E) was found to block holoenzyme assembly in isolated chloroplasts (*21*, *22*). In the study presented here, none of the substitutions at the conserved residues (Figure 2) was found to block holoenzyme assembly, including R59A and R59E substitutions at the *Chlamydomonas* residue homologous to pea Arg-53. Although it is difficult to conclude that the longer βA−βB loop of the *Chlamydomonas* small subunit is essential for holoenzyme assembly, most of the substitutions (R59A, R59E, Y67A, Y68A, and R71A) cause decreases in holoenzyme thermal stability in vitro (Figure 4), and the R59E and R71A enzymes have an associated thermal instability in vivo (Figure 3). Given that N54S and A57V substitutions in the *Chlamydomonas* βA−βB loop have also been found that improve the thermal stability of a large-subunit L290F mutant Rubisco in vivo and wild-type Rubisco in vitro (*24*), it is apparent that interactions at the interface between large subunits and the small-subunit βA−βB loop play a significant role in holoenzyme stability. Perhaps substitutions at multiple loop residues would block assembly of the eukaryotic holoenzyme.

The Y67A, Y68A, D69A, and R71A substitutions in the *Chlamydomonas* small-subunit βA−βB loop cause decreases in carboxylation catalytic efficiency (Tables 1 and 2). Similar effects on catalysis have been found in a variety of cyanobacterial small-subunit, directed-mutant enzymes (for a review, see ref *2*). However, whereas cyanobacterial large subunits expressed in the absence of small subunits retain a normal Ω value (*39*), replacement of Arg-71 with Ala in the *Chlamydomonas* small subunit causes a decrease in Ω (Table 2). Previous studies have also shown that N54S and A57V substitutions in the *Chlamydomonas* small subunit (Figure 2) can increase Ω of a large-subunit L290F mutant enzyme back to the normal value (*23*, *24*), but these small-subunit substitutions have little, if any, influence on catalysis of the wild-type enzyme (*24*). Thus, the R71A small-subunit substitution, which affects Ω directly, may provide unique information about the role of the small-subunit βA−βB loop in Rubisco function.

In the spinach Rubisco X-ray crystal structure (*8*), small-subunit residues Arg-53, Tyr-61, Tyr-62, Asp-63, and Arg-65 (Figure 2, residues 59−71 in *Chlamydomonas*) have extensive contact with each other (Figure 1A) as well as with the Rubisco large subunit. Arg-53 and Tyr-62 (Arg-59 and Tyr-68 in *Chlamydomonas*) are in contact with one large subunit, whereas Tyr-61 and Asp-63 (Tyr-67 and Asp-69 in *Chlamydomonas*) interact primarily with a second, neighboring large subunit. Arg-65 (Arg-71 in *Chlamydomonas*) interacts extensively with two large subunits (Figure 5A). It forms ionic and hydrogen bonds with Glu-223 in one large subunit and a hydrogen bond with Lys-161 in a neighboring large subunit (Figure 5A) (*8*). An atomic structure is not yet available for *Chlamydomonas* Rubisco (*40*), but one can assume that the structural interactions between the conserved small-subunit residues and the large subunits are quite similar. The six additional residues in the N-terminal half of the *Chlamydomonas* βA−βB loop (Figure 2) are likely to reside in the central solvent channel, which is encircled by the βA−βB loops of four small subunits at the top and bottom of the spinach holoenzyme (*8*). In spinach Rubisco, residues in this half of the βA−βB loop shield residues in the C-terminal half from solvent (Figure 1A). Furthermore, with regard to the large-subunit residues that are within 5 Å of the five conserved small-subunit residues, all but one (Ile-235 in spinach and Val-235 in *Chlamydomonas*) are identical in the spinach (Ω = 80) and *Chlamydomonas* (Ω = 60) enzymes. In contrast, small subunits of the cyanobacterium *Synechococcus* (Ω = 40) lack four of the five residues and contain Phe-53 in place of the spinach Arg-65 (Figure 1) (*10*). *Chlamydomonas* and spinach large subunits contain Glu-223 and Lys-161 (Figure 5A), but *Synechococcus* large subunits contain Asp-220 and Leu-158 (Figure 5B). In the holoenzyme of the eukaryotic thermophile *Galdieria partita* (Ω = 240) (*11*, *15*), small subunits contain a 30-residue extension of the C-terminus that packs in the central solvent channel. These residues may take the place of some of the missing βA−βB loop residues, but none is in contact with Ala-46, which is structurally homologous with spinach Arg-65 (Figure 5A) and *Synechococcus* Phe-53 (Figure 5B).

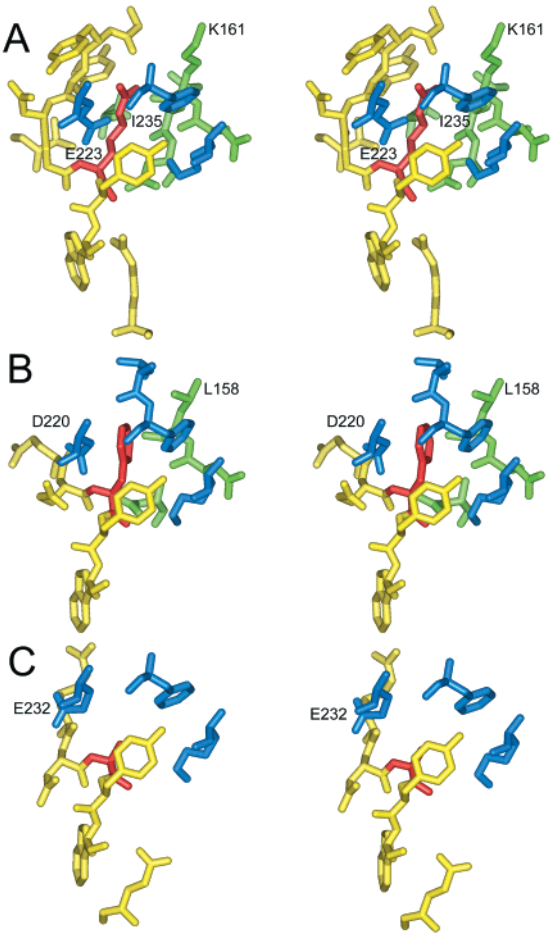

FIGURE 5: Stereoimages of residues within 5 Å of the structurally homologous (in red) Rubisco small-subunit residues Arg-65 in spinach (A), Phe-53 in *Synechococcus* (B), and Ala-46 in *Galdieria* (C). Other small-subunit residues are in yellow (spinach Val-51, Gly-60, Tyr-61, Tyr-62, Asp-63, Gly-64, Tyr-66, Trp-67, and Arg-100, *Synechococcus* Glu-51, Glu-52, Tyr-54, and Trp-55, and *Galdieria* Glu-36, Arg-44, Asn-45, Tyr-47, and Trp-48). Residues from one large subunit are in blue (spinach Lys-183, Phe-220, and Glu-223, *Synechococcus* Lys-180, Leu-216, Phe-217, and Asp-220, and *Galdieria* Lys-192, Phe-229, and Glu-232). Residues from a neighboring large subunit are in green (spinach Asp-160, Lys-161, Leu-162, Asn-163, and Ile-235 and *Synechococcus* Asp-157, Leu-158, and Asn-160). Images are derived from the X-ray crystal structures of Rubisco from spinach (8RUC), *Synechococcus* (1RBL), and *Galdieria* (1BWV) (*8*, *10*, *11*).

Residue identities and interactions relative to the *Galdieria* small-subunit Ala-46 are substantially different from those in the spinach and *Synechococcus* holoenzymes (Figure 5). Thus, there may be an interdependence between the longer βA−βB loop, Arg-65 (Arg-71 in *Chlamydomonas*), and specific residues in the large subunits of land-plant and green-algal Rubisco that may account for differences in carboxylation catalytic efficiency and Ω between long and short βA−βB-loop Rubisco enzymes. It is difficult to deduce how changes at the small-subunit−large-subunit interface can influence carboxylation catalytic efficiency and Ω at active-site residues that are 20 Å distant (*8*−*11*). Because the *Chlamydomonas* R71A mutant strain has a temperature-conditional, photosynthesis-deficient phenotype, it may be possible to select for additional, complementing substitutions as a means of identifying the most significant structural interactions (*12*, *24*, *38*).

Small subunits may have evolved due to their ability to assemble large-subunit dimers into hexadecameric holoenzymes, thereby concentrating active sites in a limited cellular compartment. Amplification of *RbcS* and *rbcL* genes during evolution also results in the production of more Rubisco holoenzyme (*25*). However, it is clear from the work presented here that at least one small-subunit region has also become intimately connected with the catalytic functions of the holoenzyme during evolution. A deeper understanding of the structure−function relationships that are responsible for retaining multiple forms of the small-subunit βA−βB loop during phylogenetic divergence may provide clues for engineering a better Rubisco enzyme.

ACKNOWLEDGMENT

We thank Chunmei Yang and John C. Szot for assistance with creating the directed-mutant enzymes. Dr. Thomas C. Taylor (Swedish University of Agricultural Sciences, Uppsala, Sweden) provided invaluable assistance in constructing and interpreting the *Synechococcus* holoenzyme crystal structure.

REFERENCES

1. Tabita, F. R. (1999) *Photosynth. Res. 60*, 1−28.
2. Spreitzer, R. J. (1999) *Photosynth. Res. 60*, 29−42.
3. Bowes, G., Ogren, W. L., and Hageman, R. H. (1971) *Biochem. Biophys. Res. Commun. 45*, 716−722.
4. Laing, W. A., Ogren, W. L., and Hageman, R. H. (1974) *Plant Physiol. 54*, 678−685.
5. Chen, Z., and Spreitzer, R. J. (1992) *Photosynth. Res. 31*, 157−164.
6. Hartman, F. C., and Harpel, M. R. (1994) *Annu. Rev. Biochem. 63*, 197−234.
7. Cleland, W. W., Andrews, T. J., Gutteridge, S., Hartman, F. C., and Lorimer, G. H. (1998) *Chem. Rev. 98*, 549−561.
8. Andersson, I. (1996) *J. Mol. Biol. 259*, 160−174.
9. Schreuder, H. A., Knight, S., Curmi, P. M. G., Andersson, I., Cascio, D., Sweet, R. M., Branden, C. I., and Eisenberg, D. (1993) *Protein Sci. 2*, 1136−1146.
10. Newman, J., and Gutteridge, S. (1993) *J. Biol. Chem. 268*, 25876−25886.
11. Sugawara, H., Yamamoto, H., Shibata, N., Inoue, T., Okada, S., Miyake, C., Yokota, A., and Kai, Y. (1999) *J. Biol. Chem. 274*, 15655−15661.
12. Spreitzer, R. J. (1998) in *The Molecular Biology of Chloroplasts and Mitochondria in Chlamydomonas* (Rochaix, J. D., Goldschmidt-Clermont, M., and Merchant, S., Eds.) pp 515−527, Kluwer Academic Publishers, Dordrecht, The Netherlands.
13. Jordan, D. B., and Ogren, W. L. (1981) *Nature 291*, 513−515.
14. Read, B. A., and Tabita, F. R. (1994) *Arch. Biochem. Biophys. 312*, 210−218.
15. Uemura, K., Anwaruzzaman, Miyachi, S., and Yokota, A. (1997) *Biochem. Biophys. Res. Commun. 233*, 568−571.
16. Kellogg, E. A., and Juliano, N. D. (1997) *Am. J. Bot. 84*, 413−428.
17. Whitney, S. M., and Andrews, T. J. (1998) *Aust. J. Plant Physiol. 25*, 131−138.
18. Getzoff, T. P., Zhu, G., Bohnert, H. J., and Jensen, R. G. (1998) *Plant Physiol. 116*, 695−702.
19. Cloney, L. P., Bekkaoui, D. R., and Hemmingsen, S. M. (1993) *Plant Mol. Biol. 23*, 1285−1290.
20. Wasmann, C. C., Ramage, R. T., Bohnert, H. J., and Ostrem, J. A. (1989) *Proc. Natl. Acad. Sci. U.S.A. 86*, 1198−1202.
21. Flachmann, R., and Bohnert, H. J. (1992) *J. Biol. Chem. 267*, 10576−10582.
22. Adam, Z. (1995) *Photosynth. Res. 43*, 143−147.

23. Chen, Z., Chastain, C. J., Al-Abed, S. R., Chollet, R., and Spreitzer, R. J. (1988) *Proc. Natl. Acad. Sci. U.S.A. 85*, 4696−4699.
24. Du, Y. C., Hong, S., and Spreitzer, R. J. (2000) *Proc. Natl. Acad. Sci. U.S.A. 97*, 14206−14211.
25. Khrebtukova, I., and Spreitzer, R. J. (1996) *Proc. Natl. Acad. Sci. U.S.A. 93*, 13689−13693.
26. Spreitzer, R. J., and Mets, L. (1981) *Plant Physiol. 67*, 565−569.
27. Yanisch-Perron, C., Vieira, J., and Messing, J. (1985) *Gene 33*, 103−119.
28. Goldschmidt-Clermont, M., and Rahire, M. (1986) *J. Mol. Biol. 191*, 421−432.
29. Deng, W. P., and Nickoloff, J. A. (1992) *Anal. Biochem. 200*, 81−88.
30. Kindle, K. L. (1990) *Proc. Natl. Acad. Sci. U.S.A. 87*, 1228−1232.
31. Spreitzer, R. J., and Chastain, C. J. (1987) *Curr. Genet. 11*, 611−616.
32. Bradford, M. M. (1976) *Anal. Biochem. 72*, 248−254.
33. Chua, N. H. (1980) *Methods Enzymol. 69*, 434−446.
34. Gotor, C., Hong, S., and Spreitzer, R. J. (1994) *Planta 193*, 313−319.
35. Jordan, D. B., and Ogren, W. L. (1981) *Plant Physiol. 67*, 237−245.
36. Spreitzer, R. J., Jordan, D. B., and Ogren, W. L. (1982) *FEBS Lett. 148*, 117−121.
37. Kuehn, G. D., and Hsu, T. C. (1978) *Biochem. J. 175*, 909−912.
38. Du, Y., and Spreitzer, R. J. (2000) *J. Biol. Chem. 275*, 19844−19847.
39. Gutteridge, S. (1991) *J. Biol. Chem. 266*, 7359−7362.
40. Yen, A., Haas, E. J., Selbo, K. M., Ross, C. R., II, Spreitzer, R. J., and Stezowski, J. J. (1998) *Acta Crystallogr. D54*, 668−670.

BI002943E